Pattern Analysis and Evaluation of Printed Circuit Boards

Masayasu Ito † Yoshinori Takeuchi † Isao Fujita † Michinori Hoshinao † Tooru Uchida ‡

† Department of Electronic Information Engineering
Tokyo University of Agriculture and Technology
2-4-16,Nakamachi,Koganei,Tokyo 184
‡ Kyouei Sangyou Co., Ltd.
1-2-6,Miyashimo,Sagamihara,Kanagawa 229

Abstract

This paper is concerned with an evaluation methodology for printed circuit boards with fine pitches, including defect analysis. The evaluation is a big issue for a mass production system. Evaluation accuracy and defect appearance rate decide yield and cost for the manufacturing lot of PC boards. We will discuss here how the inspection PC boards are compared with original pattern information, which is derived directly from an artwork, or CAD data. Topological data of the manufactured PC boards are obtained from an optical inspection system by image processings. Pattern defects are easily detected and their defect types can be also discriminated by the proposed topological comparison method. This paper describes more details about feature analysis, topological information of patterns and their features, and a fast comparison and discrimination method. Useful results and examples are presented.

Keywords: *Drawing understanding, pattern defect analysis, automatic inspection system, image processing*

1 Introduction

Printed circuit boards with fine pitches are becoming prevalent more and more so that a large number of chips and devices may be mounted on them. A human inspection system for fine pitch boards has its limitation on time and cost. Such a tedious work as verification suggests the introduction of an automatic inspection system.

Printed circuit boards are fabricated by CAD data. In conventional inspection systems, however, manufactured boards are inspected by themselves or are compared with a standard board. The conventional image comparison method is very difficult to judge whether inspection boards are completely matched with the standard board or not. The expansion and contraction method using a design rule is very effective in detecting small defects such as mouse bites, spurs, and small pinholes. It is difficult or is impossible sometimes to detect large defects such as short or open and missing patterns, however.

Powell and Carignan [1] pointed out the use of computer aided design (CAD) data for the inspection process. They suggested direct comparison of the CAD image against the products. However, it is not always necessary for an inspection board to coincide completely with the standard board as long as some specified design rules are satisfied. This work has been initiated with the aim of developing a flexible inspection system and a machine-independent defect recognition algorithm. For this purpose, we introduced topological information to the pattern analysis and to the discrimination of defects [2]. The topological representations of PCB patterns are very useful for inspection, particularly for the discrimination of large defects and the detection of missing patterns such as shorts, opens, spurious coppers, and pinholes.

Two graphs of the conductor and the insulator regions are each constructed from the skeletons of the conductor and insulator patterns, respectively both from artwork data and optically scanned inspection boards. The master graphs and inspection ones are obtained in this way.

There exist no noises on the boundary of any pattern given by CAD data, but the digitized image shows boundary noises [3,4,5], which yield extra and false skeletons. We will propose a method to exclude such a false skeleton.

Next a fast comparison technique is presented, which is to compare each branch of an inspection graph with the corresponding one of the master graph. Finally sorted branches and nodes discriminate extracted defects.

2 Master and Inspection Graphs

All patterns are drawn by the CAD data composed of primitive straight and arc lines. Necessary master information such as boundaries of patterns, skeletons, and skeletons' margin are derived from the data. The resultant skeletons become the master weighted graphs with positions and chain-coded branches.

A sequential scan is made to collect a number of divided images of the entire inspection board. The skeletons derived from mouse bites and spurs appear in many cases as relatively short branches in the resultant inspection graph, depending, of course, on how sharply they change on the boundary. Furthermore, noises on the boundary not only make us confuse with mouse bites or spurs but also yield sometimes extra skeletons, resulting in incorrect branches in the graph. Extra and false skeletons are excluded here by using an evaluation index called "convexity" with respect to the endpoint of an induced skeleton. It shows the degree of smoothness of the contour and defined as the change of degrees between the two ends of the arc on the contour, where the arc is bounded by two radii of 90 degrees apart

0-8186-4960-7/93 $3.00

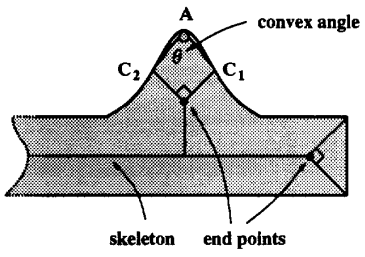

Figure 1: Definition of "convexity".

outward from the endpoint as shown in Fig. 1. When the convexity is less than 90 degrees, the skeleton with the endpoint is registered as a branch in the graph. If it is between 90 degrees and 180 degrees, the skeleton with the endpoint is regarded as a false skeleton. Since the convex angles at the endpoints in Fig. 1 are actually less than 90 degrees, the skeleton is real in this example pattern. Similarly the skeletons for each small scanning area form weighted inspection graph. Then all the skeletons of the small scanned areas are merged and become the weighted graph of the entire board.

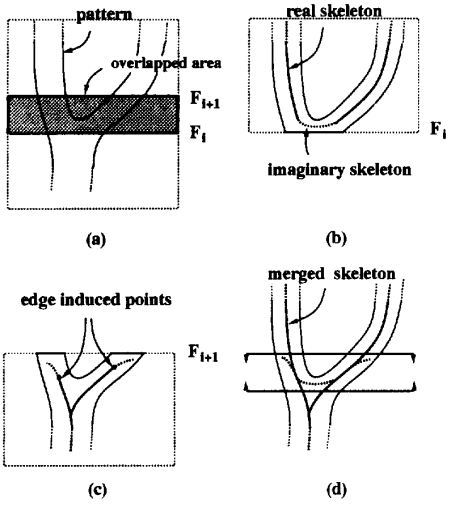

Figure 2: Illustration of the divide and merge image processings. (a)The pattern image is divided into two subimages F_i and F_{i+1}, each of which has a common overlapped area. (b)(c)Real and imaginary skeletons are obtained in each divided image. (d)True skeleton is obtained by the merge process confirming the process results in the skeleton of the entire board.

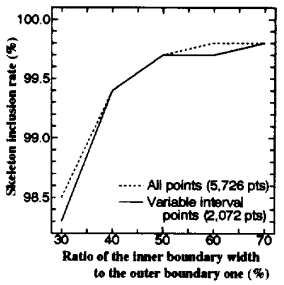

(a)

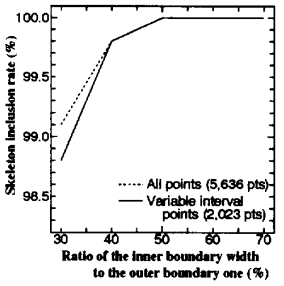

(b)

Figure 3: Skeleton inclusion rate (defect-free pattern); (a) without smoothing, (b) smoothing.

3 Pattern and Defect Analyses

Comparing inspection graph with the master graph decide the type of each inspection branch that classifies defect types. We have to note here that the skeletons of a divided subimage do not represent the true skeletons of the corresponding area, since the subimage to be processed at a time is cut at the window edge and thus, an imaginary skeleton appears near the edge. The overlapping parts of the two subimages restore the original true skeletons, as shown in Fig. 2. Note that the width of the overlapped area should be wider than the pattern width.

Skeletons are now transformed to weighted graphs. Each branch of the inspection graph is compared with the corresponding master one and is checked if it is included in the marginal area (defined as the inner region, here). Fig. 3 shows the skeleton inclusion rate versus the ratio of the inner boundary width to the outer boundary one. When the ratio becomes less than about 30 to 40 percent, the inclusion rate decreases sharply. The optimal ratio was, thus, set at about 40 percent.

For fast and efficient comparison of graphs, we employed the depth first search algorithm and a variable sampling method. Instead of tracing all the points of branches of the inspection graph, new sampling points are added to the basic sampling points explained next. Basic sampling

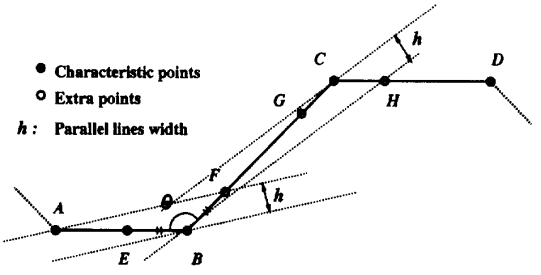

Figure 4: Basic sampling points (o and •).

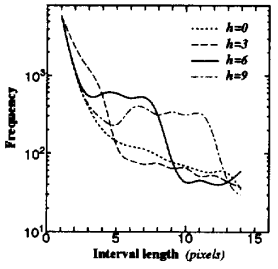

Figure 5: Histogram of interval length of skeleton.

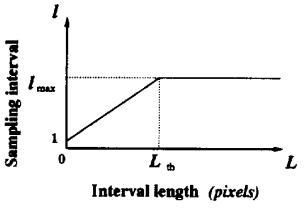

Figure 6: Variable sampling transformation curve.

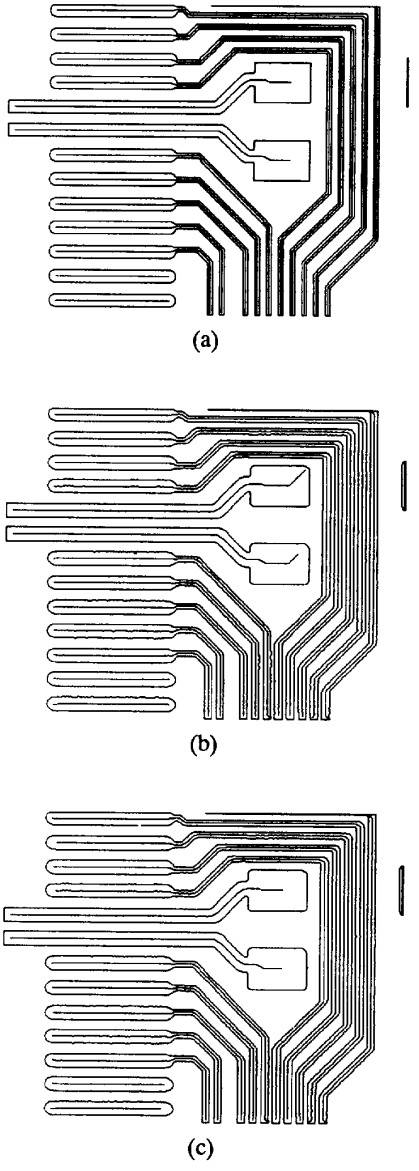

Figure 7: Outer boundaries and skeletons; (a) CAD data, (b) Optical image data (without image process), (c) Optical image data (smoothing process).

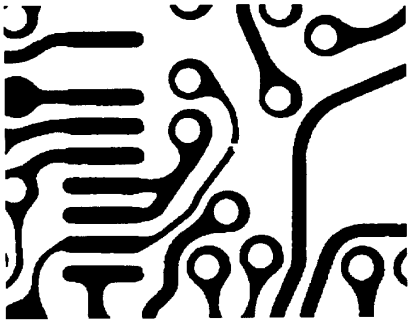

(a)

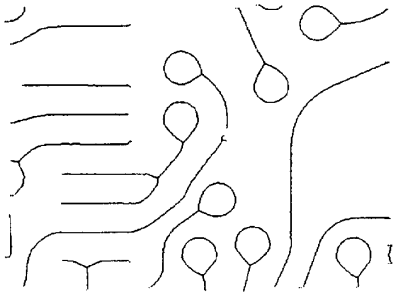

(b)

Figure 8: An example of inspection board image (a) and its skeleton (b), where the detected defect is determined as open.

points consist of the characteristic points and the extra ones so that the line connecting those points may be included in a strip of defined narrow width as shown in Fig. 4. Extra points (E,F,G,H,...) are easily obtained by simple formula;

$$\overline{BF} = \frac{h\,\overline{AB}(h\cos\theta - \sqrt{\overline{AB}^2 - h^2\sin\theta})}{h^2 - \overline{AB}^2\sin^2\theta}$$

where $\overline{AB}\sin\theta > h$. Fig 5. shows the histogram of interval length between basic sampling points in a skeleton with parameter h . h = 0 means the skeleton itself. Since h can be determined from Fig. 3, considering necessary accuracy, the next problem is how to sample the resultant inspection skeleton at variable points besides of the fixed basic sampling points. Actual sampling interval is determined by the transformation curve of Fig. 6 so that the accuracy and inspection time are compromised. Comparing Figs. 3 and 6, we set the value of L_{th} in such a way that the number of constant sampling interval(l_{max}) may become as much as possible. The constant sampling interval l_{max} is set a half of the width of fine conductor patterns. The sampling distance may decrease as the curvature of the line increases. This variable sampling process speeds up the necessary comparison time without extra works.

Fig. 7 shows the conductor patterns (outer boundaries) and skeletons. The skeleton in the original image (b) fluctuates and is not so smooth as that of CAD data. False skeletons are produced in the pad, which are excluded by the convex index as shown in (c).

Defects appear as branches of an inspection graph, which are different from those of the master one and/or not found in it. The types such as spurs, mouse bites, pinholes, excess coppers, shorts, and open are determined by their own characteristics. Figs 8(a) and (b) are each an optically scanned inspection pattern image and the resultant inspection skeleton, respectively. The skeleton in the center is disconnected and the defect is determined as open in this case.

4 Conclusions

In this report, we have presented a new automatic optical inspection system for PCB's, where CAD data are directly used for reference information. This is more powerful and flexible than conventional system, since it uses artwork data for master patterns and employs graph-theoretical rules for comparison. Almost all of spurs and mouse bites were differentiated from boundary noises by the introduction of a smooth index "convexity". Other defects were clearly identified using topological information. Related image processings and defect discrimination decision rules were also discussed.

References

[1] Julian Powell and Brian Carignan, "CAD Reference for AOI," Printed Circuit Fabrication, Vol. 12, No. 12, pp. 77-93, Dec., 1989.

[2] M. Ito and Y. Nikaido, "Recognition of Pattern Defects of Printed Circuit Board Using Topological Information," Proc. 1991 IEMT Symposium, pp. 202-206, Sept. 16-18, 1991.

[3] T. Pavlidis, "A Thinning Algorithm for Discrete Binary Images," Computer Graphics and Image Processing, 13, pp. 142-157, 1980.

[4] C. Arcelli, "Pattern Thinning by Contour Tracing," Computer Graphics and Image Processing, 17, pp. 130-144, 1981.

[5] C. Arcelli and G. Sanniti di Baja, "A Width-Independent Fast Thinning Algorithm," IEEE Trans. Pattern Analysis and Machine Intelligence, vol. PAMI-7, No. 4, pp. 463-474, 1985.